Environmental Science & Technology

Article

pubs.acs.org/est

Behavior of Aluminum, Arsenic, and Vanadium during the Neutralization of Red Mud Leachate by HCl, Gypsum, or Seawater

Ian T. Burke,*[,†] Caroline L. Peacock,[†] Cindy L. Lockwood,[†] Douglas I. Stewart,[‡] Robert J. G. Mortimer,[†] Michael B. Ward,[§] Philip Renforth,[∥] Katalin Gruiz,[⊥] and William M. Mayes[¶]

[†]Earth Surface Science Institute, School of Earth and Environment, University of Leeds, Leeds LS2 9JT, U.K.

[‡]School of Civil Engineering, University of Leeds, Leeds LS2 9JT, U.K.

[§]School of Process, Environmental and Materials Engineering, University of Leeds, Leeds LS2 9JT, U.K.

[∥]Department of Earth Sciences, University of Oxford, South Parks Road, Oxford OX3 0DP, U.K.

[⊥]Department of Applied Biotechnology and Food Science, Budapest University of Technology and Economics, St. Gellért sq. 4, 1111 Budapest, Hungary

[¶]Centre for Environmental and Marine Sciences, University of Hull, Scarborough YO11 3AZ, U.K.

Supporting Information

ABSTRACT: Red mud leachate (pH 13) collected from Ajka, Hungary is neutralized to < pH 10 by HCl, gypsum, or seawater addition. During acid neutralization >99% Al is removed from solution during the formation of an amorphous boehmite-like precipitate and dawsonite. Minor amounts of As (24%) are also removed from solution via surface adsorption of As onto the Al oxyhydroxides. Gypsum addition to red mud leachate results in the precipitation of calcite, both in experiments and in field samples recovered from rivers treated with gypsum after the October 2010 red mud spill. Calcite precipitation results in 86% Al and 81% As removal from solution, and both are nonexchangeable with 0.1 mol L^{-1} phosphate solution. Contrary to As associated with neoformed Al oxyhydroxides, EXAFS analysis of the calcite precipitates revealed only isolated arsenate tetrahedra with no evidence for surface adsorption or incorporation into the calcite structure, possibly as a result of very rapid As scavenging by the calcite precipitate. Seawater neutralization also resulted in carbonate precipitation, with >99% Al and 74% As removed from solution during the formation of a poorly ordered hydrotalcite phase and via surface adsorption to the neoformed precipitates, respectively. Half the bound As could be remobilized by phosphate addition, indicating that As was weakly bound, possibly in the hydrotalcite interlayer. Only 5−16% V was removed from solution during neutralization, demonstrating a lack of interaction with any of the neoformed precipitates. High V concentrations are therefore likely to be an intractable problem during the treatment of red mud leachates.

INTRODUCTION

Red mud is the fine fraction residue produced during aluminum extraction from bauxite in the Bayer process. The process is relatively inefficient and up to 2 tonnes of red mud are produced for every tonne of product.[1] Increasing demand for Al has seen the rate of red mud production increase, with 60−120 million tonnes being produced annually.[1] Despite efforts to find suitable after-uses for red mud,[1−10] as yet no low-cost alternative to landfill has been extensively used. Therefore, the vast majority of red mud waste is stored in land-based bauxite residue disposal areas (BRDAs).[1,11]

Due to the use of NaOH, red mud is caustic,[12,13] and water in contact with it is saline (up to 160 mS cm^{-2}) and highly alkaline (up to pH 13).[13−15] Several oxyanionic forming elements are very soluble at high pH and problematic concentrations of Al (500−1000 mg L^{-1}), As (3−5 mg L^{-1}), and V (5−10 mg L^{-1}) occur in the leachate.[14,16] The accidental release of around 1 million tonnes of red mud suspension from the Ajka BRDA, Hungary, in October 2010[17,18] focused world attention on the potential hazards associated with red mud. (Prior to the 2010 accident untreated red mud was pumped into the BRDA at 20−25% w/w solids[16] and the material released in the Oct 2010 spill contained ∼8−10% w/w solids.[19] After the accident a dry-stacking method was introduced were red mud is dewatered (∼60% w/w solids) and mixed with 10% gypsum v/v.[17]) The consequences of the spill for soil toxicity, river transport, freshwater ecology, human health, and trace metal behavior have all been recently investigated.[13,14,16,17,20−27] Research effort has also investigated the effectiveness of emergency measures taken after the spill to reduce the environmental impact of the red mud, which

Received: March 11, 2013
Revised: May 9, 2013
Accepted: May 17, 2013

 © XXXX American Chemical Society dx.doi.org/10.1021/es4010834 | Environ. Sci. Technol. XXXX, XXX, XXX−XXX

included acid dosing of residual alkaline leachates and widespread addition of large volumes of gypsum to red mud affected rivers.[14,16,26]

The chief aim of these emergency measures was to reduce pH. This removes alkalinity and reduces the solubility of oxyanions due to enhanced sorption to solids.[28] Neutralization of red mud and related leachate is commonly employed by the aluminum industry to both treat the red mud prior to disposal and as an amendment for improving prospects of establishing vegetation cover at BRDAs.[4,5,12,29−33] Dosing with mineral acids (e.g., hydrochloric or sulfuric acid) is effective, but can be costly given the large volumes required[31] and the potential handling issues involved (see Supporting Information (SI) Table S1 for indicative costs). Low-cost alternatives include gypsum and seawater addition, the latter of which is applicable in coastal refineries.[12,30,31]

Red mud leachate contains very little soluble Ca^{2+} or Mg^{2+}.[4,14] At elevated pH, any free Ca^{2+} or Mg^{2+} is rapidly removed by reaction with the high carbonate alkalinity present, forming solid carbonates.[34] Addition of gypsum to alkaline red mud releases Ca^{2+} to solution. This reacts rapidly with carbonate in the leachate (and any CO_2 that subsequently dissolves in the leachate[34,35]) to precipitate calcite.[36−38] Neutralization occurs as two moles of OH^- are consumed for every mole of calcite precipitated (eq 1;[26]) and the carbonate buffering capacity is increased. The carbonate precipitate may also provide additional sorption sites for removal of toxic trace elements[39] and excess Ca^{2+} may react directly with aluminate to form phases such as hydrocalumite ($Ca_2Al(OH)_7{\cdot}2H_2O$; eq 2;[4,31]).

$$CaSO_4{\cdot}2H_2O_{(s)} + CO_{2(aq)} + 2OH^-_{(aq)} \rightarrow CaCO_{3(s)} + SO^{2-}_{4(aq)} + 3H_2O_{(l)} \quad (1)$$

$$2CaSO_4{\cdot}2H_2O_{(s)} + Al(OH)^-_{4(aq)} + 3OH^-_{(aq)} \rightarrow Ca_2Al(OH)_7{\cdot}2H_2O_{(s)} + 2SO^{2-}_{4(aq)} + 2H_2O_{(l)} \quad (2)$$

Seawater addition works by a similar mechanism, except that the presence of Mg^{2+} leads to the formation of Mg/Al layered double hydroxide phases (e.g., hydrotalcite ($Mg_6Al_2(CO_3)(OH)_{16}{\cdot}4H_2O$); eq 3;[33]) in addition to carbonate precipitation. Layered double hydroxide minerals contain an interlayer site occupied by anions, usually carbonate or sulfate, that can also accommodate toxic oxyanions such as arsenate and vanadate, reducing their solution concentrations.[32,40]

$$6Mg^{2+}_{(aq)} + 2Al(OH)^-_{4(aq)} + 8OH^-_{(aq)} + CO^{2-}_{3(aq)} + 4H_2O_{(l)} \rightarrow Mg_6Al_2(CO_3)(OH)_{16}{\cdot}4H_2O_{(s)} \quad (3)$$

There is, however, little mechanistic understanding of trace element behavior during neutralization and a paucity of information on the stability of toxic elements sorbed by such precipitates. Indeed, lack of understanding of neutralization chemistry and leachate behavior has been highlighted as a significant knowledge gap in relation to the safe management of bauxite residues.[31]

This study therefore had the following specific objectives: (1) Investigate the changes in solution composition occurring during the neutralization of Ajka red mud leachate using HCl, gypsum, or seawater. (2) Identify the solid-phase neutralization products using electron microscopy and X-ray diffraction. (3) Determine the speciation of any solid-associated As and V using X-ray absorption spectroscopy. (4) To combine these data with chemical extractions to assess the long-term stability of toxic elements within any neoformed precipitates.

MATERIALS AND METHODS

Field Sampling and Sample Handling. In December 2010 a sediment sample (M7b) was recovered from a gypsum-amended[14,26] stream bed ∼80 km downstream from the Ajka red mud impoundment (location M7 in ref 14; in situ pH = 8.3; Lat 47°24′35 N, Long 17°20′56 E). The sample was air-dried, disaggregated using a mortar and pestle, and sieved to retain the <2 mm fraction. In May 2011 red mud leachate was collected from an open pond within cell 10 of the Ajka red mud impoundment (Lat 47°05′17 N, Long 17°29′47 E) and stored in polypropylene bottles until used.

Leachate Neutralization Experiments. All three neutralization methods used 100 mL aliquots of 0.2-μm filtered red mud leachate. After addition of the neutralizing agent, the experiments were left to equilibrate as suspensions in open containers (with foam bungs) on an orbital shaker (250 rpm) for the times indicated below. (1) HCl: An aliquot was neutralized to pH 8.3 (typical pH value recorded at sampling stations 5 km downstream of the Ajka red mud impoundment[14]) by dropwise addition of 6 mol L^{-1} HCl. Below pH 10.5 a cloudy white precipitate formed. The final pH 8.3 suspension was equilibrated for 42 days. (2) Gypsum: Gypsum ($CaSO_4{\cdot}2H_2O$) powder (3 g) was added to an aliquot of leachate and equilibrated for 63 days (gypsum addition was limited to 3 g per 100 mL so that solid-phase As and V in the precipitate were not diluted below the concentration required for XAS analysis). (3) Seawater: An aliquot was mixed with 200 mL of 35 g L^{-1} artificial seawater solution[41] following the method of ref 32. White precipitates formed immediately upon mixing and were equilibrated for 7 days. The pH was determined in all experiments using an Orion benchtop meter calibrated with pH 4, 7, and 10 buffer solutions. After equilibration, the suspensions were centrifuged for 10 min at 6000g. The supernatant was removed, filtered (0.2 μm), acidified (2% HNO_3), and analyzed as below. The precipitates were washed once in deionized water and characterized as below.

Sample Characterization. Neutralization experiment precipitates were oven-dried at 70 °C prior to X-ray powder diffraction (XRD) analysis on a Bruker D8 Advance XRD with a Cu tube. The dried precipitates, and sample M7b, were also suspended for 24 h in 0.1 mol L^{-1} Na_2HPO_4 solution at pH 8 (0.1 g in 10 mL) to determine the concentrations of anions exchangeable with phosphate.[42] Total digestions were conducted for comparison (in 2 mol L^{-1} HNO_3 for the neutralization precipitates, or microwave-assisted digestion in aqua regia/HF[43] for sample M7b). Elemental concentrations in all digests and aqueous samples were analyzed using a Perkin-Elmer Optima 5300 DV ICP-OES.

Transmission Electron Microscopy (TEM). Approximately 10 mg of dried precipitate from the HCl neutralization experiment was suspended in ethanol, placed on a Cu support grid with holey carbon support film (Agar Scientific, UK), and air-dried prior to analysis. The specimen was examined using a Philips CM200 field emission gun TEM fitted with a scanning (STEM) unit and an Oxford Instruments 80 mm^2 X-Max silicon drift X-ray detector (SDD) running Aztec software.

dx.doi.org/10.1021/es4010834 | Environ. Sci. Technol. XXXX, XXX, XXX−XXX

X-ray Absorption Spectroscopy (XAS). XANES and EXAFS data were collected at Beamline I18, Diamond Light Source, UK, in May 2012. Approximately 100 mg of each precipitate was prepared for analysis as moist pastes in Perspex holders with Kapton windows. The dried sediment sample (M7b) was prepared as a pressed pellet held in Kapton tape. XAS spectra were collected at the V and As K-edges (5465 and 11867 eV, respectively). Standard spectra were collected from a range of laboratory chemicals, aqueous solutions (1000 mg L^{-1}), vanadate sorbed to $Al(OH)_3$, and a hydrous Ca arsenate precipitate ($Ca_3(AsO_4)_2{\cdot}xH_2O$). All XANES spectra were averaged and normalized using Athena v0.8.061 and plotted for samples and standards. V K-edge EXAFS samples spectra were affected by irresolvable interferences with the La L_3-edge observed at 5483 eV, therefore, these spectra were not analyzed. As K-edge EXAFS spectra from all samples were interference free and background subtracted using PySpline v1.1. EXAFS spectra were then fitted in DLexcurv v1.0[44] to model clusters (SI Figure S1) representing various As binding environments relevant to the precipitates recovered from the leachate neutralization experiments. See SI Sections 1 and 2 for detailed descriptions and protocols.

RESULTS

Solution Chemistry. The red mud leachate (Table 1) contained slightly higher trace element concentrations compared to water samples collected in Dec 2010[14] and had broadly similar composition to leachates reported from other BDRAs.[15,32,45] Neutralization resulted in pH reduction from pH 13.1 in the raw leachate to pH 8.3 after HCl titration, pH 9.8 after gypsum treatment, and pH 9.7 after mixing with seawater. In general, leachate neutralization substantially removed Al from solution, however, the gypsum treatment was somewhat less effective (86% removed) than either the HCl or seawater treatments (99.7−99.9% removed). A small amount of As was removed in the HCl treatment (24%) but significantly more was removed during gypsum and seawater neutralization (74−81%). Very little B, Cr, Ga, Mo, or V was removed during HCl neutralization (5−12%), and gypsum treatment also resulted in relatively small removal of these elements (4−22%). Seawater treatment removed small amounts of B, Mo, and V (10−14%), but removed 41% of the Cr and almost all Ga (99%) from solution.

Table 1. Concentration of Selected Oxyanion-Forming Elements in Red Mud Leachate before and after Neutralization Experiments (0.2-μm Filtered)[a]

		supernatant concentration (μg L^{-1})		
determinand	red mud leachate (μg L^{-1})	HCl treated[b]	gypsum treated[c]	seawater treated[d]
Al	352000	1220 (99.7)	49100 (86)	300 (99.9)
As	8140	6220 (24)	1550 (81)	2120 (74)
B	1690	1490 (12)	1550 (8)	1530 (10)
Cr	188	169 (10)	167 (11)	110 (41)
Ga	2250	1990 (10)	1750 (22)	24 (99)
Mo	11600	10450 (9)	11030 (4)	10400 (10)
V	15600	14800 (5)	13100 (16)	13500 (14)
pH	13.1	8.3	9.8	9.7

[a]Percent removed shown in parentheses. [b]Dosage ~5 mL L^{-1}. [c]Dosage 30 g L^{-1}. [d]Dosage 2 L L^{-1}. Values adjusted for dilution.

XRD Characterization. The HCl neutralized precipitate contained XRD peaks (Figure 1) consistent with poorly ordered dawsonite ($NaAl(OH)_2CO_3$).[46] The gypsum neutralized sample contained only calcite peaks, with gypsum not detected in the XRD pattern. Likewise, calcite was the major phase and gypsum was not detected in the M7b stream sediment sample. However, a range of natural fluvial sediment minerals were also detected in M7b, including quartz (SiO_2), muscovite ($KAl_2(AlSi_3O_{10})(F,OH)_2$), chlorite ($(Mg_5Al)(AlSi_3)O_{10}(OH)_8$), and microcline ($KAlSi_3O_8$). XRD patterns from the seawater neutralized precipitate contained peaks consistent with poorly ordered hydrotalcite ($Mg_6Al_2(CO_3)(OH)_{16}{\cdot}4(H_2O)$[47]), calcite, aragonite ($CaCO_3$), and gypsum.

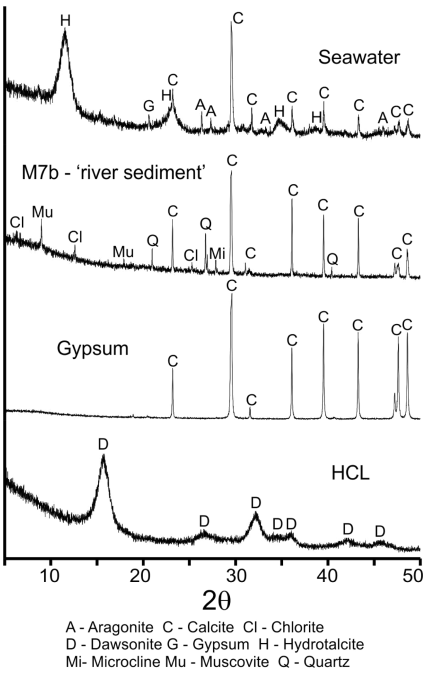

Figure 1. XRD patterns collected from dried precipitates recovered from leachate neutralization experiments and the M7b river sediment. Where present, the large calcite peak at ~29° 2θ has been truncated to allow vertical exaggeration to enhance the visibility of smaller peaks.

TEM Analysis. TEM imaging of the precipitate formed by HCl neutralization (Figure 2), shows that it was composed of 5−30 nm particles in 100−500 nm aggregates that were found to be largely amorphous by selected area electron diffraction (SAED). Semiquantitative EDX analysis of the particles found that the molar O/Al ratio was 1.91 ± 0.15 and the Na/Al ratio was 0.10 ± 0.05. Several elements (including As, C, Ca, Cl, K, P, S, and Si) were also detected as minor peaks in EDX spectra. In EDX maps (SI Figure S2) Al, O, and As were evenly distributed throughout the aggregates but Na distribution was patchy.

Phosphate Extractions. Aluminum was largely not extractable by phosphate from any of the precipitates or M7b (Table 2). Some As was extracted by phosphate leaching of the HCl (19%) and seawater (49%) precipitates. In contrast, less than 5% of the As present was phosphate extractable from either the gypsum precipitate or M7b. Moderate amounts (10−27%) of V were extracted from the HCl, gypsum, or M7b samples by phosphate addition, and 47% of the V present was extracted from the seawater precipitate.

dx.doi.org/10.1021/es4010834 | Environ. Sci. Technol. XXXX, XXX, XXX−XXX

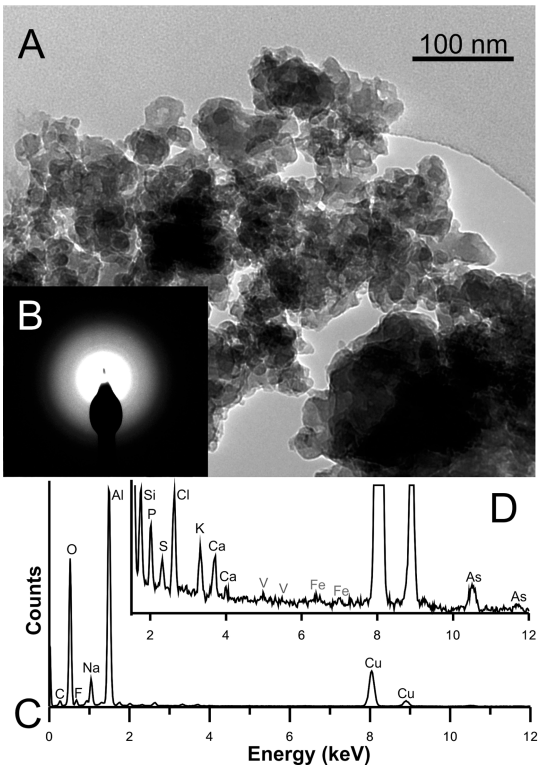

Figure 2. (A) Low-resolution bright field (S)TEM image of the leachate precipitate produced by HCl neutralization; (B) its selected area electron diffraction pattern; (C) the EDX spectra collected from the precipitate; and (D) 40× vertical exaggeration of the 1.5−12 keV region of the EDX spectra showing the minor peaks detected. The positions of V and Fe peaks are indicated but were not autodetected by the acquisition software. Cu peaks are due to the TEM grid used to support the sample.

Table 2. Concentrations of Al, As, and V Found in Leachate Neutralization Precipitates and the M7b River Sediment, and the Percentage Found to Be Extractable in 0.1 mol L^{-1} Na_2HPO_4 Solution at pH 8 (Shown in Parentheses)

	concentration (mg kg^{-1}) (% extracted by Na_2HPO_4)		
sample ID	Al	As	V
HCl	137300 (0.6)	988 (19)	181 (10)
gypsum	17100 (0.1)	344 (5)	150 (27)
M7b sediment	57100 (0.1)	197 (<4)[a]	135 (24)
seawater	49850 (<0.1)[a]	694 (49)	204 (47)

[a]< % based on limit of detection by ICP-OES.

Vanadium XANES Analysis. The V K-edge XANES spectra (Figure 3) collected from the HCl and gypsum neutralization precipitates, and the M7b stream sediment, all have prominent pre-edge peaks between 5470 and 5470.3 eV (all energy values are quoted to ±0.20 eV) with normalized intensities between 0.57 and 0.71. The main absorption edges ($E_{1/2}$ = point where absorption reaches 50% of the normalized absorption) are between 5480.4 and 5481.7 eV. The vanadate sorbed to $Al(OH)_3$ spectrum also has a pre-edge peak at 5470.2 eV, a normalized intensity of 0.64, and $E_{1/2}$ = 5480.3 eV. The spectrum collected from the seawater neutralization precipitate has a pre-edge at 5470.2 eV, with a normalized intensity of 1.12, and $E_{1/2}$ = 5482.4 eV. A summary of the spectral information extracted from all samples and standards is shown in Table 3.

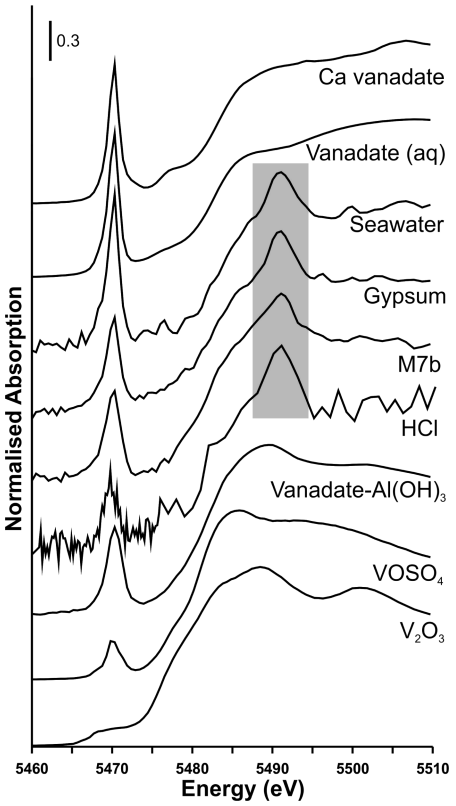

Figure 3. Normalized V K-edge XANES spectra collected from the moist pastes recovered from leachate neutralization experiments, the dried M7b stream sediment, and standards containing V^{3+}, V^{4+}, and V^{5+}. The vanadate spectrum is from a 1000 mg L^{-1} aqueous solution in 0.1 mol L^{-1} NaOH. The gray box denotes where the white line peak of the La L_3-edge is visible in spectra from experimental samples and the M7b stream sediment.

Table 3. Pre-Edge Peak Position, Normalized Pre-Edge Peak Intensity, and Main Edge Position Determined from the V K-edge XANES Spectra Shown in Figure 3[a]

sample/compound	valence	pre-edge peak (eV)	normalized intensity	main edge, $E_{1/2}$ (eV)
V_2O_3	3+	5468.0	0.05	5476.4
$VOSO_4 \cdot xH_2O$	4+	5470.0	0.30	5478.8
vanadate sorbed to $Al(OH)_3$	5+	5470.2	0.64	5480.3
HCl precipitate	5+	5470.0	0.57	5481.3
M7b sediment	5+	5470.2	0.66	5480.4
gypsum precipitate	5+	5470.3	0.71	5481.7
seawater precipitate	5+	5470.2	1.12	5482.4
vanadate (aq)	5+	5470.1	1.02	5481.8
calcium meta-vanadate	5+	5470.2	1.06	5482.2

[a]Energy values are quoted ±0.2 eV; normalized intensity values are quoted ±0.1.

Arsenic XAS Analysis. The As K-edge XANES spectra (SI Figure S3) collected from the neutralized precipitates and M7b sediment confirm that only As^{5+} is detectable in all samples. The arsenic K-edge EXAFS spectra collected from the gypsum precipitate and M7b (Figure 4) both have similar coordination environments with spectra fitted with 4 oxygen backscatters at 1.65−1.74 Å (Table 4). An additional peak identified in the Fourier transforms at around 2.8 Å is entirely attributed to

dx.doi.org/10.1021/es4010834 | Environ. Sci. Technol. XXXX, XXX, XXX−XXX

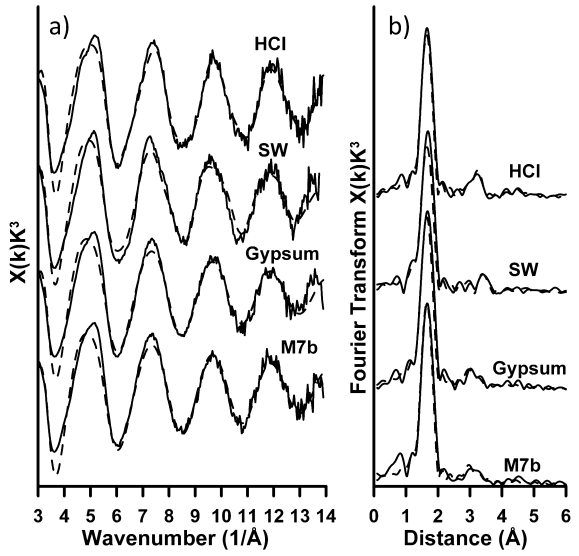

Figure 4. (A) Background subtracted As K-edge EXAFS spectra collected from the leachate precipitates and the M7b river sediment. (B) Corresponding Fourier transforms calculated from EXAFS spectra. Dashed lines represent DLexcurv V1.0 model fits using the parameters listed in Table 4.

multiple scattering within the arsenate tetrahedron.[48] The fits to these spectra could not be statistically improved (reduced Chi^2) by including an additional shell of either Al or Ca backscatterers at ~3.2 or 3.4−3.6 Å, respectively. EXAFS data collected from the HCl and seawater precipitate were best fit with an additional shell of ~2 Al backscatters at around 3.2 or 3.3−3.4 Å, respectively, with a resultant 40−50% improvement in reduced Chi^2 compared to the one shell model (Table 4).

DISCUSSION

HCl Neutralization. The precipitate from the acid neutralization experiment removed >99% Al from solution and contained dawsonite. The formation of dawsonite from alkaline Al-rich liquors has been observed when the molar Na/Al ratio is greater than 3; below this value boehmite (AlO(OH)) is predicted to dominate.[46] The molar Na/Al ratio of Ajka red mud leachate was ~1,[14] and EDX analysis of the HCl precipitate showed that the molar O/Al ratio was within error of that expected for boehmite (i.e., 2). Boehmite was not observed in XRD patterns, but SAED showed the precipitate was largely amorphous. It is therefore likely that early precipitation of an amorphous boehmite-like Al oxyhydroxide in the acid neutralization experiment depleted aqueous Al to the point where dawsonite precipitation became favorable (the molar Na/Al after neutralization was >100[14]). The molar Na/Al ratio in the precipitate (0.1) is only 10% of that expected for pure dawsonite (1.0); therefore dawsonite is in fact only a minor component of the acid neutralization precipitate.

Arsenic is only partially removed from solution during HCl neutralization. EXAFS analysis of the precipitate indicates that As is most likely present as arsenate adsorbed to the neoformed Al-oxyhydroxides in bidentate corner-sharing complexes (see SI Figure S1b). Arsenate in such inner-sphere surface adsorption complexes is only partially susceptible to ligand exchange,[5,42] and most of the adsorbed As is therefore not remobilized by phosphate addition. Arsenate adsorption to Al-oxyhydroxides via bidentate corner-sharing complexes has been reported

Table 4. As K-edge EXAFS Fits Where *N* is the Occupancy (± 25%), R is the Interatomic Distance (± 0.02 Å for the First Shell, ± 0.05 Å for Outer Shells), $2\sigma^2$ is the Debye-Waller Factor (± 25%), and *R* and Reduced χ^2 are the Least Squares Residual and the Reduced Chi^2 Goodness of Fit Parameters, Respectively[a]

					goodness of fit	
sample	shell	*N*	R (Å)	$2\sigma^2$ (Å^2)	*R* (%)	reduced χ^2
M7b	O	1	1.71	0.003	24	7.7
	O	1	1.67	0.006		
	O	1	1.67	0.006		
	O	1	1.67	0.006		
gypsum	O	1	1.72	0.004	24	8.2
	O	1	1.68	0.006		
	O	1	1.67	0.006		
	O	1	1.67	0.006		
HCl: fit with 4 O	O	1	1.69	0.003	24	7.3
	O	1	1.68	0.005		
	O	1	1.68	0.006		
	O	1	1.67	0.005		
HCl: fit with 4 O and 2 Al (shown on Figure 3)	O	1	1.70	0.002	21	4.5
	O	1	1.66	0.006		
	O	1	1.64	0.007		
	O	1	1.68	0.002		
	Al	1	3.21	0.012		
	Al	1	3.20	0.010		
seawater: fit with 4 O	O	1	1.69	0.003	28	13.7
	O	1	1.71	0.002		
	O	1	1.61	0.003		
	O	1	1.71	0.002		
seawater: fit with 4 O and 2 Al (shown on Figure 3)	O	1	1.69	0.003	27	6.9
	O	1	1.70	0.002		
	O	1	1.61	0.003		
	O	1	1.71	0.002		
	Al	1	3.37	0.002		
	Al	1	3.27	0.008		

[a]Four As−O bonds have been considered separately to allow for multiple scattering within the AsO_4 tetrahedron. *N* values were held constant during the fitting.

previously for similar HCl neutralization experiments.[16] The difference in this study was that the leachate was filtered at 0.2 μm prior to neutralization, and as a result the amount of As adsorption was much lower (24% rather than 94% when the leachate was unfiltered;[16]). This highlights the importance of red mud particulates (chiefly hematite) in determining the fate of As when red mud leachate is neutralized with HCl.

At the pH of the raw leachate, vanadate is predicted to dominate V aqueous speciation.[49−51] Almost no V was removed from solution during HCl neutralization (the reverse of that previously observed with unfiltered leachate[16]). The V K-edge XANES spectrum collected from this sample has quite poor data quality (Figure 3); nevertheless, the XANES data shows the absorption edge energy ($E_{1/2}$) is similar to those of the V^{5+} containing standards, and above that of most V^{4+} containing compounds.[52−54] When this spectrum is interpreted using the system of Charaund et al.[52] (based on the detailed observation of pre-edge peak intensity and energy position; see SI section 3 for detailed explanation), the HCl precipitate data plot closely to the data from vanadate adsorbed to oxide and hydroxide surfaces,[40,55,56] including the vanadate-Al(OH)$_3$

dx.doi.org/10.1021/es4010834 | Environ. Sci. Technol. XXXX, XXX, XXX−XXX

standard produced in this study (SI Figure S4). Therefore, the V K-edge XANES data for the HCl neutralized sample are consistent with vanadate adsorption to the neoformed precipitates.

Gypsum Neutralization. During gypsum neutralization aqueous Ca^{2+} concentration will be limited by gypsum solubility (Ksp = $10^{-4.60}$ [28]). Ca^{2+} is removed from the leachate by calcite precipitation. At alkaline pH, rapid dissolution of atmospheric CO_2 provides CO_3^{2-} to support this reaction. In the gypsum neutralization experiment essentially full conversion of gypsum to calcite was observed. No gypsum is apparent in XRD patterns collected from the solid residue, and there is also no evidence for the presence of the Ca-aluminate phases that have been reported previously.[4,31] However, it should be noted that Al was almost completely removed from solution and Al oxyhydroxide phases are predicted to be oversaturated in mineral saturation modeling (SI Tables S2 and S3); therefore, neoformed Al-phases must be present and are likely to be amorphous or not detectable by XRD (i.e., less than ~5% w/w).

Sample M7b was taken about 2 months after the Ajka red mud spill from a location on the Marcal River that received large volumes of gypsum in response to the spill. This location became noted for the resulting carbonate hardpans on the stream bed.[14,23,26] The XRD pattern collected from M7b was dominated by calcite along with minor amounts of other minerals typical of river sediments. No gypsum (or red-mud-derived phases such as hematite) was detectable in the spectrum. Thus the gypsum amended leachate residue and the M7b river sediment appear to be experimental and field derived products of essentially the same phenomenon, namely gypsum addition to Ajka red mud leachate.

Arsenic was largely removed from solution during gypsum neutralization. Mineral saturation modeling (SI Tables S2 and S3) of the equilibrium leachate composition after the addition of gypsum, indicates that the solution is not oversaturated with respect to Ca-arsenate phases during the initial reaction. Arsenic K-edge EXAFS analysis of spectra collected from both the gypsum precipitate and M7b samples shows that the local As coordination environment is consistent with the tetrahedral arsenate structure. There is no evidence for any contribution to these spectra from additional shells of backscattering atoms at longer distances, such as the As−Ca linkages observed in Ca-arsenates (SI Figure S5;[39,57]). Arsenate in apparently outer-sphere sorption complexes should be partially susceptible to ligand exchange,[5,42] yet the sorbed As was not remobilized by phosphate addition to either the gypsum precipitate or M7b. EXAFS spectra collected of calcite crystals grown slowly in the presence of arsenate contain strong evidence for As−Ca backscatters due to the direct substitution of arsenate for carbonate in the calcite lattice.[39,58] Gypsum addition to alkaline red mud leachate, however, induces very rapid carbonate precipitation (possibly via high surface area amorphous intermediates[59]). During rapid precipitation, arsenate is likely to become associated with positively charged carbonate surfaces due to charge compensating surface sorption[39] and may then be protected from further exchange reactions by incorporation into the calcite precipitate in noncrystallographic sites (as observed for chromate−calcite coprecipitates[60]).

V removal from the red mud leachate during gypsum treatment is only slightly greater than during HCl addition. XANES analysis indicates that solid-associated V is likely to be present as vanadate surface adsorption complexes, possibly associated with the calcite precipitate.

Seawater Neutralization. Seawater addition to red mud leachate provides aqueous Ca^{2+}. This promoted the formation of calcium carbonate (aragonite and calcite) in much the same way as gypsum addition. Mg^{2+} is also present and this promoted the formation of the Al/Mg layered double hydroxide phase hydrotalcite, which accounts for the high degree of Al removal observed. Layered double hydroxides contain an interlayer site that is accessible to many different oxyanions, including carbonate, phosphate, and sulfate; and has been predicted as a host phase for trace elements such As and V present as soluble oxyanions in red mud leachates.[32,40,61]

Arsenic was largely removed from solution during seawater neutralization, and EXAFS analysis revealed that solid-associated As was in a coordination environment similar to that in the HCl precipitate. However the As−Al bond lengths discovered were slightly longer (3.3−3.4 Å) than those in the HCl precipitate and those commonly found when As is associated with aluminum oxide surfaces (3.2 Å[62]). Moreover, a significant amount of the solid-phase As was phosphate exchangeable. Taken together this indicates the As is present in a surface adsorption environment with weaker As−Al bonding than the As-adsorbed HCl precipitate. In turn this may indicate As sorption at the interlayer site of the neoformed hydrotalcite, however, the exact bonding environment for As in hydrotalcite has not been determined.

Similar to HCl and gypsum addition, V is not extensively removed from solution during seawater treatment, which is consistent with previous seawater neutralization studies.[32] The V K-edge XANES spectrum from the seawater neutralized precipitate (Table 3) is within error of the data collected from the calcium metavanadate standard. However, mineral speciation modeling of the seawater/leachate mixture (SI Tables S2 and S3) does not predict oversaturation with respect to Ca-vanadate. Furthermore, much of the solid-associated V was found to be exchangeable with phosphate, which should not occur for Ca-vanadate precipitates. Sorption of vanadate at the interlayer site of neoformed hydrotalcite has been proposed to account for V removal from solution during seawater neutralization of Bayer liquors.[32,33,61] Therefore, sorption of vanadate to the hydrotalcite interlayer site may account for the small amounts of V removal observed.

Implications for Bauxite Residue Management. All three neutralization methods used are successful in reducing the pH of red mud leachate and removing Al from solution. Depending on the method, Al removal is achieved via the precipitation of various Al oxyhydroxides, hydroxycarbonates, or layered double hydroxides. In these precipitates, Al is not phosphate exchangeable and the Al concentrations in the neutralized leachate are controlled by the solubility of the solid products, which at between pH 5 and 10 is generally low.[28,32,63] The effect of neutralization on other trace elements present is more variable. Arsenic can be substantially removed from solution using all three methods, but in the case of HCl addition additional sorption surfaces must be present to achieve high degrees of removal.[16] For HCl and seawater treatments, As sorption is achieved through formation of inner-sphere complexes (most likely associated with neoformed precipitates). However, some As remobilization can be achieved by anion exchange with phosphate. Gypsum addition, however, appears to incorporate As nonexchangeably into neoformed calcite precipitates. This result is consistent with reports on the

use of gypsum to treat rivers following the Ajka red mud spill, where increased concentrations of weak acid extractable As are found in neoformed calcite hardpans.[14,26] V is not substantially removed from solution by any of the neutralization methods studied. Indeed, persistent V solubility was an intractable problem in waters affected by the Ajka spill;[14,16] although there is some evidence that the presence of additional sorption sites helps to reduce aqueous V concentration.[16] A number of other trace elements, B, Cr, Ga, and Mo are also not removed during neutralization (with the exception of Ga during seawater treatment).

In recent years, other methods of red mud neutralization using CO_2 and SO_2 from power station flue gas have been investigated as carbon sequestration/waste minimization methods.[10,64,65] Several biological methods have also been tested for pH reduction, including direct bacterial action (bicarbonate generation)[66,67] and placing vegetation cover over red mud stock piles (leaching of plant organic acids into the red mud is thought to reduce pH[4,29,68]). These studies have suggested that neutralization methods involving divalent cation addition (e.g., gypsum or seawater addition) are more effective in controlling toxic metal concentrations than acid dosing.[4,32] The results of this study show that neutralization of red mud leachate by any method is an important step in reducing the overall burden of alkalinity and soluble toxic elements on the aqueous environment, especially Al and As. Gypsum neutralization can probably be considered the most effective method used in this study, as both As and Al were nonexchangeably sorbed, and the precipitated carbonate buffers against further pH changes. The estimated amounts of gypsum required ($\sim$ 1200 t a^{-1}) to treat leachate that is potentially generated at a site such as the Ajka BDRA are also relatively modest (see SI Section S4 for detailed calculations and assumptions).

Extrapolation of the treated aqueous metal and metalloid concentrations from small-scale experiments to bulk water quality and subsequent comparison with aquatic life standards must be done with utmost caution. However, if we assume a 100-fold dilution factor of the treated leachate once discharged into a receiving stream (which is consistent with comparisons of baseflow measurements taken from the upper Torna Creek[14] with the leachate generation estimates above (SI Section S4)), the Al concentrations found in the gypsum treatment would be in breach of the strictest aquatic life standards[69] by a factor of 6, and V concentrations by a factor of 2. As such, it would be likely that some additional polishing treatment of the leachate would be required prior to discharge, for example through a deployment of a treatment wetland, which is effective for Al and V removal in the pH range of the neutralized leachate.[37,70]

■ ASSOCIATED CONTENT

Ⓢ Supporting Information

Detailed XAS methods, red mud leachate composition, mineral saturation indexes, molecular cluster diagrams, additional TEM images and XAS data. This material is available free of charge via the Internet at http://pubs.acs.org.

■ AUTHOR INFORMATION

Corresponding Author

*E-mail: i.t.burke@see.leeds.ac.uk; phone: +44 113 3437532; fax: +44 113 3435259.

Notes

The authors declare no competing financial interest.

■ ACKNOWLEDGMENTS

We acknowledge funding from the UK Natural Environment Research Council (grant NE/I019468/1) and thank Diamond Light Source for access to beamline I18 (grant SP7525) that contributed to the results presented here. Thanks to Tina Geraki (Diamond Light Source) for support during synchrotron time, Lesley Neve and Janice Littlewood (University of Leeds) for XRD analysis, and Bob Knight (University of Hull) for ICP analysis. István Csonki (Central Danubian Water and Environment Authority) is thanked for site access and orientation.

■ REFERENCES

(1) Power, G.; Graefe, M.; Klauber, C. Bauxite residue issues: I. Current management, disposal and storage practices. *Hydrometallurgy* **2011**, *108* (1−2), 33−45.

(2) Altundogan, H. S.; Altundogan, S.; Tumen, F.; Bildik, M. Arsenic removal from aqueous solutions by adsorption on red mud. *Waste Manage.* **2000**, *20* (8), 761−767.

(3) Courtney, R. G.; Harrington, T. Growth and nutrition of *Holcus lanatus* in bauxite residue amended with combinations of spent mushroom compost and gypsum. *Land Degrad. Dev.* **2012**, *23* (2), 144−149.

(4) Courtney, R. G.; Kirwan, L. Gypsum amendment of alkaline bauxite residue - Plant available aluminium and implications for grassland restoration. *Ecol. Eng.* **2012**, *42*, 279−282.

(5) Genc-Fuhrman, H.; Tjell, J. C.; McConchie, D. Adsorption of arsenic from water using activated neutralized red mud. *Environ. Sci. Technol.* **2004**, *38* (8), 2428−2434.

(6) Liu, Y.; Naidu, R.; Ming, H. Red mud as an amendment for pollutants in solid and liquid phases. *Geoderma* **2011**, *163* (1−2), 1−12.

(7) Somlai, J.; Jobbagy, V.; Kovacs, J.; Tarjan, S.; Kovacs, T. Radiological aspects of the usability of red mud as building material additive. *J. Hazard. Mater.* **2008**, *150* (3), 541−545.

(8) Summers, R. N.; Guise, N. R.; Smirk, D. D. Bauxite residue (red mud) increases phosphorous retention in sandy soil catchments in Western Australia. *Fert. Res.* **1993**, *34* (1), 85−94.

(9) Wang, S.; Ang, H. M.; Tade, M. O. Novel applications of red mud as coagulant, adsorbent and catalyst for environmentally benign processes. *Chemosphere* **2008**, *72* (11), 1621−1635.

(10) Yadav, V. S.; Prasad, M.; Khan, J.; Amritphale, S. S.; Singh, M.; Raju, C. B. Sequestration of carbon dioxide (CO(2)) using red mud. *J. Hazard. Mater.* **2010**, *176* (1−3), 1044−1050.

(11) Grafe, M.; Klauber, C. Bauxite residue issues: IV. Old obstacles and new pathways for in situ residue bioremediation. *Hydrometallurgy* **2011**, *108* (1−2), 46−59.

(12) Hind, A. R.; Bhargava, S. K.; Grocott, S. C. The surface chemistry of Bayer process solids: a review. *Colloids Surf., A* **1999**, *146* (1−3), 359−374.

(13) Ruyters, S.; Mertens, J.; Vassilieva, E.; Dehandschutter, B.; Poffijn, A.; Smolders, E. The Red Mud Accident in Ajka (Hungary): Plant Toxicity and Trace Metal Bioavailability in Red Mud Contaminated Soil. *Environ. Sci. Technol.* **2011**, *45* (4), 1616−1622.

(14) Mayes, W. M.; Jarvis, A. P.; Burke, I. T.; Walton, M.; Feigl, V.; Klebercz, O.; Gruiz, K. Dispersal and Attenuation of Trace Contaminants Downstream of the Ajka Bauxite Residue (Red Mud) Depository Failure, Hungary. *Environ. Sci. Technol.* **2011**, *45* (12), 5147−5155.

(15) Czop, M.; Motyka, J.; Sracek, O.; Szuwarzynski, M. Geochemistry of the Hyperalkaline Gorka Pit Lake (pH > 13) in the Chrzanow Region, Southern Poland. *Water, Air, Soil Pollut.* **2011**, *214* (1−4), 423−434.

(16) Burke, I. T.; Mayes, W. M.; Peacock, C. L.; Brown, A. P.; Jarvis, A. P.; Gruiz, K. Speciation of Arsenic, Chromium, and Vanadium in Red Mud Samples from the Ajka Spill Site, Hungary. *Environ. Sci. Technol.* **2012**, *46* (6), 3085−3092.

(17) Adam, J.; Banvolgyi, G.; Dura, G.; Grenerczy, G.; Gubek, N.; Gutper, I.; Simon, G.; Szegfalvi, Z.; Szekacs, A.; Szepvolgyi, J.; Ujlaky, E. *The Kolontár Report. Causes and Lessons from the Red Mud Disaster*;Javor, B., Hargitai, M., Eds.; Greens/European Free Alliance Parliamentary Group in the European Parliament and LMP - Politics Can Be Different: Budapest, 2011; p 156.

(18) Reeves, H. J., Wealthall, G., and Younger, P. L. *Advisory Visit to the Bauxite Processing Tailings Dam near Ajka, Vesprem County, Western Hungary*; British Geological Survey: Keyworth, UK, 2011.

(19) Szépvölgyi, J. A Chemical Engineer's View of the Red Mud Disaster. *Nachr. Chem.* **2011**, *59*, 5−7.

(20) Czovek, D.; Novak, Z.; Somlai, C.; Asztalos, T.; Tiszlavicz, L.; Bozaki, Z.; Ajtai, T.; Utry, N.; Filep, A.; Bari, F.; Petak, F. Respiratory consequences of red sludge dust inhalation in rats. *Toxicol. Lett.* **2012**, *209* (2), 113−120.

(21) Gelencser, A.; Kovats, N.; Turoczi, B.; Rostasi, A.; Hoffer, A.; Imre, K.; Nyiro-Kosa, I.; Csakberenyi-Malasics, D.; Toth, A.; Czitrovszky, A.; Nagy, A.; Nagy, S.; Acs, A.; Kovacs, A.; Ferincz, A.; Hartyani, Z.; Posfai, M. The Red Mud Accident in Ajka (Hungary): Characterization and Potential Health Effects of Fugitive Dust. *Environ. Sci. Technol.* **2011**, *45* (4), 1608−1615.

(22) Gruiz, K.; Feigl, V.; Klebercz, O.; Anton, A.; Vaszita, E. Environmental Risk Assessment of Red Mud Contaminated Land in Hungary. In *GeoCongress 2012: State of the Art and Practice in Geotechnical Engineering*; American Society of Civil Engineers: Reson, VA, 2012.

(23) Klebercz, O.; Mayes, W. M.; Anton, A. D.; Feigl, V.; Jarvis, A. P.; Gruiz, K. Ecotoxicity of fluvial sediments downstream of the Ajka red mud spill, Hungary. *J. Environ. Monit.* **2012**, *14* (8), 2063−71.

(24) Milacic, R.; Zuliani, T.; Scancar, J. Environmental impact of toxic elements in red mud studied by fractionation and speciation procedures. *Sci. Total Environ.* **2012**, *426*, 359−365.

(25) Rédey, A. The red mud disaster of Ajka in Hungary and its consequences. In *4th EUCHeMS Chemistry Congress*; Prague, Czech Republic, 2012.

(26) Renforth, P.; Mayes, W. M.; Jarvis, A. P.; Burke, I. T.; Manning, D. A. C.; Gruiz, K. Contaminant mobility and carbon sequestration downstream of the Ajka (Hungary) red mud spill: The effects of gypsum dosing. *Sci. Total Environ.* **2012**, *421*−*422*, 253−259.

(27) Scholl, K.; Szovenyi, G. Planktonic Rotifer Assemblages of the Danube River at Budapest after the Red Sludge Pollution in Hungary. *Bull. Environ. Contam. Toxicol.* **2011**, *87* (2), 124−128.

(28) Langmuir, D. *Aqueous Environmental Chemistry*; Prentice-Hall Inc.: Upper Saddle River, NJ, 1997.

(29) Courtney, R. G.; Timpson, J. P. Nutrient status of vegetation grown in alkaline bauxite processing residue amended with gypsum and thermally dried sewage sludge - A two-year field study. *Plant Soil* **2004**, *266* (1), 187−194.

(30) Courtney, R. G.; Timpson, J. P. Reclamation of fine fraction bauxite processing residue (red mud) amended with coarse fraction residue and gypsum. *Water, Air. Soil Pollut.* **2005**, *164* (1−4), 91−102.

(31) Grafe, M.; Power, G.; Klauber, C. Bauxite residue issues: III. Alkalinity and associated chemistry. *Hydrometallurgy* **2011**, *108* (1−2), 60−79.

(32) Palmer, S. J.; Frost, R. L. Characterization of Bayer Hydrotalcites Formed from Bauxite Refinery Residue Liquor. *Ind. Eng. Chem. Res.* **2011**, *50* (9), 5346−5351.

(33) Palmer, S. J.; Frost, R. L.; Nguyen, T. Hydrotalcites and their role in coordination of anions in Bayer liquors: Anion binding in layered double hydroxides. *Coord. Chem. Rev.* **2009**, *253* (1−2), 250−267.

(34) Renforth, P.; Manning, D. A. C.; Lopez-Capel, E. Carbonate precipitation in artificial soils as a sink for atmospheric carbon dioxide. *Appl. Geochem.* **2009**, *24* (9), 1757−1764.

(35) Burke, I. T.; Mortimer, R. J. G.; Palaniyandi, S.; Whittleston, R. A.; Lockwood, C. L.; Ashley, D. J.; Stewart, D. I. Biogeochemical Reduction Processes in a Hyper-Alkaline Leachate Affected Soil Profile. *Geomicrobiol. J.* **2012**, *29* (9), 769−779.

(36) Roadcap, G. S.; Kelly, W. R.; Bethke, C. M. Geochemistry of extremely alkaline (pH > 12) ground water in slag-fill aquifers. *Ground Water* **2005**, *43* (6), 806−816.

(37) Mayes, W. M.; Younger, P. L.; AumÃnier, J. Buffering of alkaline steel slag leachate across a natural wetland. *Environ. Sci. Technol.* **2006**, *40* (4), 1237−1243.

(38) Mayes, W. M.; Younger, P. L.; AumÃnier, J. Hydrogeochemistry of alkaline steel slag leachates in the UK. *Water, Air, Soil Pollut.* **2008**, *195* (1−4), 35−50.

(39) Alexandratos, V. G.; Elzinga, E. J.; Reeder, R. J. Arsenate uptake by calcite: Macroscopic and spectroscopic characterization of adsorption and incorporation mechanisms. *Geochim. Cosmochim. Acta* **2007**, *71* (17), 4172−4187.

(40) Goh, K. H.; Lim, T. T.; Dong, Z. L. Removal of arsenate from aqueous solution by nanocrystalline Mg/Al layered double hydroxide: Sorption characteristics, prospects, and challenges. *Water Sci. Technol.* **2010**, *61* (6), 1411−1417.

(41) Subow, N. N. *Oceanographical Tables. U.S.S.R*; Oceanogr. Institute, Hydro-meteorol. Com: Moscow, 1931; p 208.

(42) Manning, B. A.; Goldberg, S. Modeling competitive adsorption of arsenate with phosphate and molybdate on oxide minerals. *Soil Sci. Soc. Am. J.* **1996**, *60* (1), 121−131.

(43) USEPA. *Microwave Assisted Acid Digestion of Siliceous and Organically Based Matrices; USEPA Method 2052*; Washington, DC, 1996.

(44) Tomic, S.; Searle, B. G.; Wander, A.; Harrison, N. M.; Dent, A. J.; Mosselmans, J. F. W.; Inglesfield, J. E. *New Tools for the Analysis of EXAFS: The DL_EXCURV Package; CCLRC Technical Report DL-TR-2005-001*; Daresbury, UK, 2005.

(45) Khaitan, S.; Dzombak, D. A.; Lowry, G. V. Chemistry of the Acid Neutralization Capacity of Bauxite Residue. *Environ. Eng. Sci.* **2009**, *26* (5), 873−881.

(46) Alvarez-Ayuso, E.; Nugteren, H. W. Synthesis of Dawsonite: A method to treat the etching waste streams of the aluminium anodising industry. *Water Res.* **2005**, *39* (10), 2096−2104.

(47) Kanezaki, E. Thermal behavior of the hydrotalcite-like layered structure of Mg and Al-layered double hydroxides with interlayer carbonate by means of in situ powder HTXRD and DTA/TG. *Solid State Ionics* **1998**, *106* (3−4), 279−284.

(48) Sherman, D. M.; Randall, S. R. Surface complexation of arsenie(V) to iron(III) (hydr)oxides: Structural mechanism from ab initio molecular geometries and EXAFS spectroscopy. *Geochim. Cosmochim. Acta* **2003**, *67* (22), 4223−4230.

(49) Wehrli, B.; Stumm, W. Vanadyl in natural waters - Adsorption and hydrolysis promote oxygenation. *Geochim. Cosmochim. Acta* **1989**, *53* (1), 69−77.

(50) Evans, H. T. Molecular structure of isopoly complex ion decavanadate ($V_{10}O_{28}^{6-}$). *Inorg. Chem.* **1966**, *5* (6), 967.

(51) Cornelis, G.; Poppe, S.; Van Gerven, T.; Van den Broeck, E.; Ceulemans, M.; Vandecasteele, C. Geochemical modelling of arsenic and selenium leaching in alkaline water treatment sludge from the production of non-ferrous metals. *J. Hazard. Mater.* **2008**, *159* (2−3), 271−279.

(52) Chaurand, P.; Rose, J.; Briois, V.; Salome, M.; Proux, O.; Nassif, V.; Olivi, L.; Susini, J.; Hazemann, J.-L.; Bottero, J.-Y. New methodological approach for the vanadium K-edge X-ray absorption near-edge structure interpretation: Application to the speciation of vanadium in oxide phases from steel slag. *J. Phys. Chem. B* **2007**, *111* (19), 5101−5110.

(53) Liu, R. S.; Cheng, Y. C.; Gundakaram, R.; Jang, L. Y. Crystal and electronic structures of inverse spinel-type $LiNiVO_4$. *Mater. Res. Bull.* **2001**, *36* (7−8), 1479−1486.

(54) Wong, J.; Lytle, F. W.; Messmer, R. P.; Maylotte, D. H. K-edge absorption-spectra of selected vanadium compounds. *Phys. Rev. B* **1984**, *30* (10), 5596−5610.

(55) Bronkema, J. L.; Bell, A. T. Mechanistic studies of methanol oxidation to formaldehyde on isolated vanadate sites supported on MCM-48. *J. Phys. Chem. C* **2007**, *111* (1), 420−430.

(56) Tanaka, T.; Yamashita, H.; Tsuchitani, R.; Funabiki, T.; Yoshida, S. X-ray absorption (EXAFS XANES) study of supported vanadium-oxide catalysts - Structure of surface vanadium oxide species on silica and gamma-alumina at a low-level of vanadium loading. *J. Chem. Soc.-Faraday Trans. I* **1988**, *84*, 2987−2999.
(57) Luo, Y.; Giammar, D. E.; Huhmann, B. L.; Catalono, J. G. Speciation of selenium, arsenic, and zinc in class C fly ash. *Energy Fuels* **2011**, *25*, 2980−2987.
(58) Winkel, L. H. E.; Casentini, B.; Bardelli, F.; Voegelin, A.; Nikolaidis, N. P.; Charlet, L. Speciation of arsenic in Greek travertines: Co-precipitation of arsenate with calcite. *Geochim. Cosmochim. Acta* **2013**, *106* (0), 99−110.
(59) Rodriguez-Blanco, J. D.; Shaw, S.; Benning, L. G. The kinetics and mechanisms of amorphous calcium carbonate (ACC) crystallization to calcite, via vaterite. *Nanoscale* **2011**, *3* (1), 265−271.
(60) Tang, Y.; Elzinga, E. J.; Jae Lee, Y.; Reeder, R. J. Coprecipitation of chromate with calcite: Batch experiments and X-ray absorption spectroscopy. *Geochim. Cosmochim. Acta* **2007**, *71* (6), 1480−1493.
(61) Palmer, S. J.; Frost, R. L. Use of Hydrotalcites for the Removal of Toxic Anions from Aqueous Solutions. *Ind. Eng. Chem. Res.* **2010**, *49* (19), 8969−8976.
(62) Ladeira, A. C. Q.; Ciminelli, V. S. T.; Duarte, H. A.; Alves, M. C. M.; Ramos, A. Y. Mechanism of anion retention from EXAFS and density functional calculations: Arsenic (V) adsorbed on gibbsite. *Geochim. Cosmochim. Acta* **2001**, *65* (8), 1211−1217.
(63) Benezeth, P.; Palmer, D. A.; Anovitz, L. M.; Horita, J. Dawsonite synthesis and reevaluation of its thermodynamic properties from solubility measurements: Implications for mineral trapping of CO(2). *Geochim. Cosmochim. Acta* **2007**, *71* (18), 4438−4455.
(64) Khaitan, S.; Dzombak, D. A.; Lowry, G. V. Mechanisms of Neutralization of Bauxite Residue by Carbon Dioxide. *J. Environ. Eng.* **2009**, *135* (6), 433−438.
(65) Yamada, K.; Harato, F. SO_2 removal from waste-gas by red mud slurry pilot test and operation results of the plant. *Kagaku Kogaku Ronbunshu* **1982**, *8*, 32−38.
(66) Hamdy, M. K.; Williams, F. S. Bacterial amelioration of bauxite residue waste of industrial alumina plants. *J. Ind. Microbiol. Biotechnol.* **2001**, *27* (4), 228−233.
(67) Krishna, P.; Reddy, M. S.; Patnaik, S. K. *Aspergillus tubingensis* reduces the pH of the bauxite residue (Red mud) amended soils. *Water, Air, Soil Pollut.* **2005**, *167* (1−4), 201−209.
(68) Courtney, R. G.; Jordan, S. N.; Harrington, T. Physico-chemical changes in bauxite residue following application of spent mushroom compost and gypsum. *Land Degrad. Dev.* **2009**, *20* (5), 572−581.
(69) Buchman, M. F. S. W. *NOAA Screening Quick Reference Tables*; Office of Response and Restoration Division, National Oceanic and Atmospheric Administration: Washington, DC, 2006; p 34.
(70) Mayes, W. M.; Aumonier, J.; Jarvis, A. P. Preliminary evaluation of a constructed wetland for treating extremely alkaline (pH 12) steel slag drainage. *Water Sci. Technol.* **2009**, *59* (11), 2253−2263.